

Planar Hall Plateau in Magnetic Weyl Semimetals

Lei Li,^{1,2,*} Chaoxi Cui,^{1,2,*} Run-Wu Zhang,^{1,2} Zhi-Ming Yu,^{1,2,3,†} and Yugui Yao^{1,2,3,‡}

¹Centre for Quantum Physics, Key Laboratory of Advanced Optoelectronic Quantum Architecture and Measurement (MOE), School of Physics, Beijing Institute of Technology, Beijing, 100081, China

²Beijing Key Lab of Nanophotonics & Ultrafine Optoelectronic Systems, School of Physics, Beijing Institute of Technology, Beijing, 100081, China

³International Center for Quantum Materials, Beijing Institute of Technology, Zhuhai, 519000, China

Despite the rapid progress in the study of planar Hall effect (PHE) in recent years, all the previous works only showed that the PHE is connected to local geometric quantities, such as Berry curvature. Here, *for the first time*, we point out that the PHE in magnetic Weyl semimetals is directly related to a global quantity, namely, the Chern number of the Weyl point. This leads to a remarkable consequence that the PHE observation predicted here is robust against many system details, including the Fermi energy. The main difference between non-magnetic and magnetic Weyl points is that the latter breaks time-reversal symmetry \mathcal{T} , thus generally possessing an energy tilt. Via semiclassical Boltzmann theory, we investigate the PHE in generic magnetic Weyl models with energy tilt and arbitrary Chern number. We find that by aligning the magnetic and electric fields in the same direction, the trace of the PHE conductivity contributed from Berry curvature and orbital moment is proportional to the Chern number and the energy tilt of the Weyl points, resulting in previously undiscovered quantized PHE plateau by varying Fermi energy. We further confirm the existence of PHE plateaus in a more realistic lattice model without \mathcal{T} symmetry. By proposing a new quantized physical quantity, our work not only provides a new tool for extracting the topological character of the Weyl points but also suggests that the interplay between topology and magnetism can give rise to intriguing physics.

Introduction.— The band topology, referring to the topological properties of the electronic band structure of materials, have attracted considerable attention in the field of condensed matter physics [1, 2]. Generally, one can utilize the geometric quantities, which are locally defined at each momentum point in the Brillouin zone (BZ), to describe it. Some common geometric quantities include Berry curvature and its dipole [1, 3–7], Berry-connection polarizability and its dipole [8–13], and quantum metric [14–18]. However, the essential aspect of topological states is that they host (at least) a global quantity, i.e. topological charge [19–23], which also is used to characterize and distinguish topological states. For example, the integral of the Berry curvature over a 2D closed surface in momentum space may result in Chern number [24]. More importantly, in stark contrast to local geometric quantities and general physical observations, global topological quantities are integers and are robust to many material details [25, 26].

Recently, various Hall effects, including nonlinear Hall effects [8–11, 27–44] and many kinds of planar Hall effect (PHE) [45–56], have been proposed and demonstrated to have a close relationship with geometric quantities. Since the geometric quantities are significantly enhanced around band degeneracies, these unconventional Hall effects are widely investigated in topological semimetals [57–66]. As aforementioned, the existence of a global

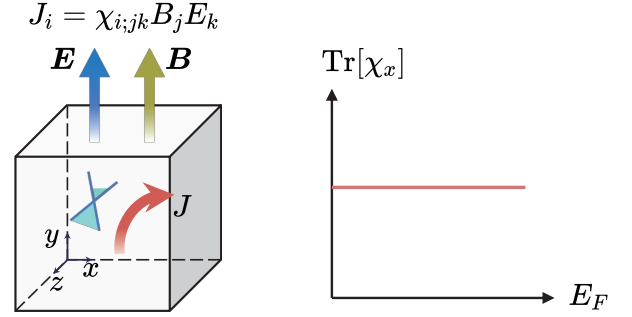


FIG. 1. Sketch of PHE in topological Weyl semimetals with magnetic and electric fields aligned in the same direction. In this case, the trace of the PHE conductivity $\text{Tr}[\chi_x] = \sum_j \chi_{x;jj}$ is in direct proportion to the Chern number of the WP, and is robust against many system details, leading to a flat plateau at low energy.

quantity rather than local geometric quantities is the most remarkable feature of topological states. Unfortunately, the PHEs have not yet been reported to be associated with a global quantity.

In this work, we show that the PHE in magnetic Weyl semimetals is directly linked to the topological charge (Chern number) of the Weyl point. In PHE, the magnetic field, the driving electric field, and the transverse Hall current are in the same plane [58, 67], as illustrated in Fig. 1, which is completely different from the setup in ordinary Hall effect. Initially, PHE was attributed to system anisotropy [45]. Subsequent findings unveiled that the Berry curvature also affects PHE, leading to a surge in research on PHE in topological Weyl semimetals [68–

* These authors contributed equally to this work

† zhiming_yu@bit.edu.cn

‡ ygyao@bit.edu.cn

75]. Recently, Li *et al.* [67] found that the PHE resulting from orbital moment is comparable with that from Berry curvature. However, a common observation is that the PHE mechanisms in these studies are independent of any global quantity.

Here, based on semiclassical Boltzmann theory, we investigate PHE in the charge- n (with n an integer) Weyl points (C- n WPs) with energy tilt, which is a common feature for magnetic WPs. For magnetic WPs, the leading order of PHE generally is linear due to the breaking of time reversal symmetry (\mathcal{T}) [67]. The linear PHE conductivity contains six terms, with one term contributed by Lorentz force and the remaining terms originating from geometric quantities, i.e. Berry curvature and orbital moment. Remarkably, by aligning the magnetic and electric fields in the same direction (see Fig. 1), we demonstrate that the trace of the PHE conductivity contributed by Berry curvature and orbital moment ($\text{Tr}[\chi_i]$ with $i = x, y, z$) is quantized for all the C- n WPs resulting from the global topology of the WP, and then is robust against many material details. The analytical derivation of $\text{Tr}[\chi_i]$ shows that the $\text{Tr}[\chi_i]$ is fully determined by the Chern number and the energy tilt of the WPs. This feature becomes increasingly more precise when the Fermi energy approaches the WPs. By unveiling a novel magnetotransport phenomenon directly related to the global quantities of WP in magnetic Weyl semimetals, our work deepens the understanding on the PHE, and provides a promising method to detect the topological charge and the energy tilt of the WPs.

Linear PHE conductivity.— Generally, the PHE conductivity under weak fields can be obtained from semiclassical equations of motion [1] and the Boltzmann transport equation [76]. Here, we focus on the setup that the driving electric field \mathbf{E} and the magnetic field \mathbf{B} are aligned in the same direction, *i.e.*, $\mathbf{E} \parallel \mathbf{B}$ (see Fig. 1). For the three-dimensional magnetic systems, the leading terms of the PHE that have topological origin are linearly dependent on both \mathbf{E} and \mathbf{B} , expressed as [67]

$$\mathbf{J}_i = \chi_{i;jj} B_j \mathbf{E}_j, \quad (1)$$

where \mathbf{J} is the current density and $\chi_{i;jj}$ denotes the PHE conductivity. The PHE conductivity $\chi_{i;jk}$ is a third-order tensor, and the $\chi_{i;jj}$ in Eq. (1) denotes a diagonal element of the matrix χ_i . $\chi_{i;jj}$ can be further decomposed into the following five parts [67]:

$$\chi_{i;jj} = \chi_{i;jj}^{(1)} + \chi_{i;jj}^{(2)} + \chi_{i;jj}^{(3)} + \chi_{i;jj}^{(4)} + \chi_{i;jj}^{(5)}, \quad (2)$$

with

$$\begin{aligned} \chi_{i;jj}^{(1)} &= -e^3 \tau \int [d\mathbf{k}] v_i v_j \Omega_j \partial_\varepsilon f_k^0, \\ \chi_{i;jj}^{(2)} &= e^3 \tau \int [d\mathbf{k}] v_j (\mathbf{v} \cdot \boldsymbol{\Omega}) \partial_\varepsilon f_k^0, \\ \chi_{i;jj}^{(3)} &= e^3 \tau \int [d\mathbf{k}] v_i (\mathbf{v} \cdot \boldsymbol{\Omega}) \partial_\varepsilon f_k^0, \\ \chi_{i;jj}^{(4)} &= -e^2 \tau \int [d\mathbf{k}] v_i \partial_{k_j} m_j \partial_\varepsilon f_k^0, \\ \chi_{i;jj}^{(5)} &= -e^2 \tau \int [d\mathbf{k}] v_j \partial_{k_i} m_j \partial_\varepsilon f_k^0. \end{aligned} \quad (3)$$

Here, $\int [d\mathbf{k}] \equiv -\frac{1}{(2\pi)^3 \hbar} \int d^3 k$, ε is the band energy, $\mathbf{v} = \partial_{\mathbf{k}} \varepsilon / \hbar$ denotes the velocity, $\boldsymbol{\Omega}$ and \mathbf{m} respectively are the Berry curvature and the orbital moment, τ is the relaxation time, and f_k^0 is the Fermi-Dirac distribution. The electron charge is taken as $-e$ (*i.e.*, $e > 0$).

An analysis of Eq. (3) reveals two crucial features of the topological PHE conductivities $\chi_{i;jj}$. First, all the five PHE conductivities linearly depend on τ . Thus, they can be easily extracted in experiments [77, 78], as the contributions from intrinsic Hall effect and Lorentz force are even functions of τ [67]. This linear dependence also indicates that the topological PHE conductivities only appear in the magnetic systems, as \mathcal{T} reverses \mathbf{J} , \mathbf{B} and τ , but keeps \mathbf{E} invariant.

Second, one observes that the trace of the matrix $\chi_i^{(1)}$ equals to $-\chi_{i;jj}^{(3)}$, *i.e.*, $\text{Tr}[\chi_i^{(1)}] = \sum_j \chi_{i;jj}^{(1)} = -\chi_{i;jj}^{(3)}$, and $\text{Tr}[\chi_i^{(3)}] = 3\chi_{i;jj}^{(3)}$. Thus, the trace of χ_i is

$$\text{Tr}[\chi_i] \equiv \sum_j \chi_{i;jj} = \text{Tr}[\chi_i^{(2)}] + \frac{2}{3} \chi_{i;jj}^{(3)} + \chi_{i;jj}^{(4)} + \chi_{i;jj}^{(5)}, \quad (4)$$

in which the contribution from Berry curvature and orbital moment are $\text{Tr}[\chi_i^{(2)}] = \text{Tr}[\chi_i^{(2)}] + \frac{2}{3} \chi_{i;jj}^{(3)}$ and $\text{Tr}[\chi_i^{(4)}] = \text{Tr}[\chi_i^{(4)} + \chi_i^{(5)}]$, respectively.

Third, the topological PHE conductivities $\chi_{i;jj}$ are determined by the properties of the Fermi surface, due to the presence of $\partial_\varepsilon f_k^0$. It has been demonstrated that the geometry quantities at the Fermi surface have a significant influence on the PHE conductivities [67–69]. However, the Fermi surface may also possess global quantities. The influence of the global quantities on the PHE conductivities has not been investigated. Since the most famous global quantity that may be hosted by a 2D Fermi surface is the Chern number (\mathcal{C}), here we focus on the topological PHE conductivities $\chi_{i;jj}$ of generic magnetic WPs with different Chern numbers.

Linear WP and scaling analysis.— Before studying a generic Weyl model with arbitrary Chern number, it is instructive to begin with a conventional (linear) WP with $|\mathcal{C}| = 1$, which has a linear dispersion along all the directions in momentum space [79]. Due to the absence of \mathcal{T} symmetry, the magnetic WP generally has an energy

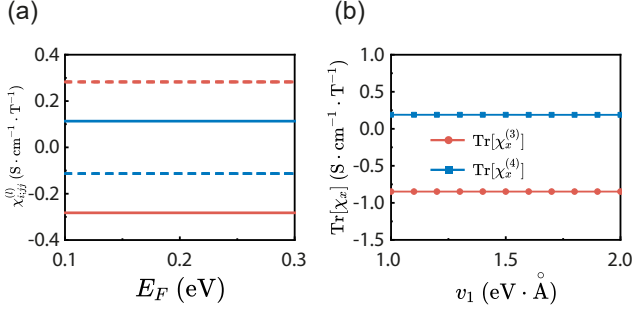


FIG. 2. Variation of PHE conductivity with (a) Fermi level E_F and (b) Fermi velocity v_1 . In panel (a), the red and blue lines correspond to the $\chi_{x;y}^{(3)}$ and $\chi_{x;xx}^{(4)}$, respectively. Solid lines represent results for $w_x > 0$ and dashed lines for $w_x < 0$. We set $|w_x| = 0.2 \text{ eV} \cdot \text{\AA}$, and $v_1 = 1.0 \text{ eV} \cdot \text{\AA}$ in (a), and set $w_x = 0.2 \text{ eV} \cdot \text{\AA}$ and $E_F = 200 \text{ meV}$ in (b). We also set $\tau = 0.1 \text{ ps}$ in all calculations.

tilt. For linear WP, the leading term for the energy tilt is also linear. Thus, a general Hamiltonian for the magnetic linear WP can be written as [79]

$$\mathcal{H}_1 = w_x k_x + v_1 \mathbf{k} \cdot \boldsymbol{\sigma}, \quad (5)$$

with w_x and v_1 the real parameters respectively representing the energy tilt and Fermi velocity of the WP, and $\boldsymbol{\sigma}$ being the Pauli matrix. Here, without loss of generality, we have set the energy tilt to be along k_x direction. We also assume $|w_x| < |v_1|$ to guarantee the Fermi surface of the WP close [80, 81]. It is easy to know that this model (5) exhibits a linear dispersion and exhibits a Chern number $\mathcal{C} = \text{Sign}(v_1)$.

A striking feature of the system that exhibits same order of dispersion along all the directions is that its various important properties can be obtained by applying a simple scaling analysis [82]. For this model (5), we consider a scaling transformation in momentum and energy: $\mathbf{k} \rightarrow \lambda \mathbf{k}$ and $E_F \rightarrow \lambda E_F$, where λ is a real number. Due to the linear feature of Eq. (5), one has $\mathcal{H}_1(\lambda \mathbf{k}) = \lambda \mathcal{H}_1(\mathbf{k})$ and $\varepsilon(\lambda \mathbf{k}) = \lambda \varepsilon(\mathbf{k})$. Note that the velocity and the eigenstates of the system are invariant under the scaling, *i.e.*, $v(\lambda \mathbf{k}) = v(\mathbf{k})$ and $|u_{n,\lambda \mathbf{k}}\rangle = |u_{n,\mathbf{k}}\rangle$. Then, the Berry curvature and orbital moment transform as $\boldsymbol{\Omega}_{\lambda \mathbf{k}} = \lambda^{-2} \boldsymbol{\Omega}_{\mathbf{k}}$ and $\mathbf{m}_{\lambda \mathbf{k}} = \lambda^{-1} \mathbf{m}_{\mathbf{k}}$, respectively.

As a consequence, for all the five PHE conductivities in Eq. (3), we have

$$\chi_{i;jj}^{(l)}(\lambda E_F) = \chi_{i;jj}^{(l)}(E_F), \quad (6)$$

indicating that the $\chi_{i;jj}^{(l)}$ ($l = 1, \dots, 5$) is a quantity that surprisingly has no dependence on Fermi energy, leading to a PHE plateau in energy space, as shown in Fig. 2(a). Further numerical calculations show that the trace of the PHE conductivity $\text{Tr}[\chi_i^{(l)}]$ is also robust to the absolute value of v_1 , and is only dependent on its sign [see Fig.

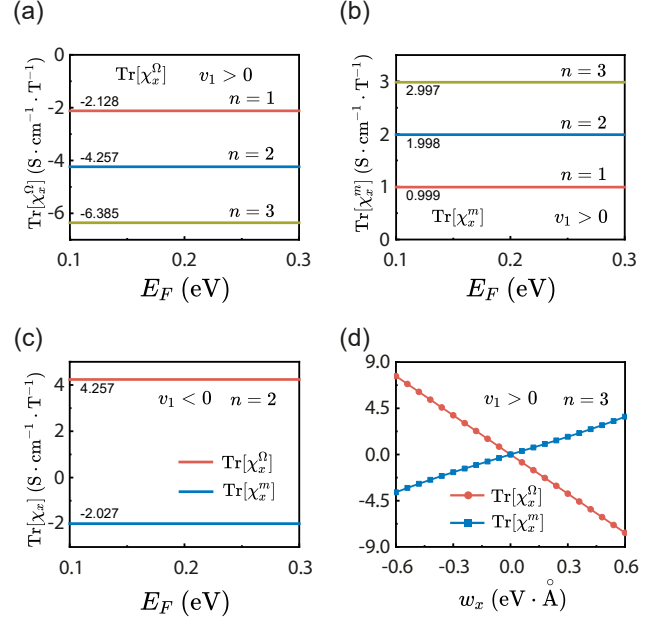


FIG. 3. Variation of PHE conductivity (a) $\text{Tr}[\chi_x^{\Omega}]$ and (b) $\text{Tr}[\chi_x^m]$ with Fermi level for $n = 1, 2, 3$ when $v_1 > 0$. The corresponding value of η and β in Table I are $\eta = 0.474 \text{ S} \cdot \text{\AA} \cdot \text{cm}^{-1} \cdot \text{eV}^{-1} \cdot \text{T}^{-1}$ and $\beta = 0.112$. (c) Variation of $\text{Tr}[\chi_x^{\Omega}]$ and $\text{Tr}[\chi_x^m]$ with Fermi level for $n = 2$ when $v_1 < 0$. The corresponding $\beta = 0.143$. (d) Variation of $\text{Tr}[\chi_x^{\Omega}]$ and $\text{Tr}[\chi_x^m]$ with energy tilt w_x for $n = 3$ when $v_1 > 0$. We set $w_x = 0.5 \text{ eV} \cdot \text{\AA}$ in (a-c), $v_1 = 1.0 \text{ eV} \cdot \text{\AA}$, $c_+ = 0.3 \text{ eV} \cdot \text{\AA}^n$, and $c_- = 1.2 \text{ eV} \cdot \text{\AA}^n$ in (a), (b) and (d); $v_1 = -0.9 \text{ eV} \cdot \text{\AA}$, $c_+ = 0.4 \text{ eV} \cdot \text{\AA}^n$ and $c_- = 1.0 \text{ eV} \cdot \text{\AA}^n$ in (c). We also set $E_F = 200 \text{ meV}$ in (d) and $\tau = 0.1 \text{ ps}$ in all calculations.

2(b)], which is reminiscent of the Chern number of the WP $\mathcal{C} = \text{Sign}(v_1)$. Notice that in the field of condensed matter physics, it is quite rare for an *observable* to have such a robust feature. All these results indicate that the PHE conductivity $\text{Tr}[\chi_i^{(l)}]$ in WP should be more nontrivial than previously understood. Besides, from symmetry analysis, one knows that the value of the PHE plateau would be reversed when the sign of w_x is changed, as both w_x and $\chi_{i;jj}^{(l)}$ are anti-symmetric under \mathcal{T} symmetry. This is confirmed by our numerical calculations, as shown in Fig. 2(a).

Beyond linear model.— We then discuss the trace of PHE conductivity $\text{Tr}[\chi_i]$ in a generic magnetic WP with arbitrary Chern number, for which the Hamiltonian reads [83, 84],

$$\mathcal{H}_2 = w_x k_x + \begin{bmatrix} v_1 k_x & c_+ k_+^n + c_- k_-^n \\ c_+ k_-^n + c_- k_+^n & -v_1 k_x \end{bmatrix}, \quad (7)$$

with $k_{\pm} = k_y \pm ik_z$, n an integer (which can be 1, 2, and 3 in crystals), and c_{\pm} a real parameter. The Chern number of this WP is $\mathcal{C} = n \times \text{Sign}(v_1)$ for $|c_+| > |c_-|$ and is $\mathcal{C} = -n \times \text{Sign}(v_1)$ for $|c_+| < |c_-|$. Again, we require the WP to be a type-I point with $|w_x| < |v_1|$. For $n \neq 1$,

TABLE I. The PHE conductivity $\text{Tr}[\chi_i^{(l)}]$ of a generic WP model (7) where the energy tilt is along k_x direction. Here, \mathcal{C} is the Chern number of the WP, $\eta = e^3\tau/(12\pi^2\hbar^3)$, and $\beta = [-2\alpha^3 + 3\alpha + 3(\alpha^2 - 1)\text{arctanh}\alpha]/\alpha^3$. w_x and $\alpha = |w_x/v_1| < 1$ denote the absolute and relative energy tilt, respectively.

	Berry curvature			orbital moment	
	$l = 1$	$l = 2$	$l = 3$	$l = 4$	$l = 5$
$\text{Tr}[\chi_x^{(l)}]/\eta$	$-3w_x\mathcal{C}$	$3w_x\mathcal{C}$	$9w_x\mathcal{C}$	$(-2 - \beta)w_x\mathcal{C}$	$(-2 - \beta)w_x\mathcal{C}$
$\text{Tr}[\chi_y^{(l)}]/\eta$	0	$3w_x\mathcal{C}$	0	0	0
$\text{Tr}[\chi_z^{(l)}]/\eta$	0	$3w_x\mathcal{C}$	0	0	0

the WP has a linear dispersion along k_x , but a nonlinear dispersion along other directions. Thus, it can not be investigated by scaling analysis.

The numerical results of $\text{Tr}[\chi_i^{\Omega(m)}]$ based on Hamiltonian \mathcal{H}_2 (7) are presented in Fig. 3. A remarkable observation is that while $\chi_{i,jj}^{\Omega(m)}$ is no longer independent of Fermi energy, due to the loss of linear dispersion, the trace, i.e. $\text{Tr}[\chi_i^{\Omega(m)}]$ remain robust against E_F , as shown in Fig. 3(a-c). More than that, the plateau of $\text{Tr}[\chi_i^{\Omega(m)}]$ is completely not effected by the nonlinear dispersion and the band anisotropy induced by the parameters c_{\pm} (see Fig. 3). Again, we find that the PHE plateau is sensitive to the value of n and the sign of v_1 , i.e., the Chern number of the WP. Moreover, we find that $\text{Tr}[\chi_i^{\Omega}]$ linearly depend on the energy tilt w_x , while $\text{Tr}[\chi_i^m]$ shows a linear dependence on w_x when w_x is small, but increasingly deviates it when w_x increases, as shown in Fig. 3(d). All these results strongly suggest that the trace of the PHE conductivity $\text{Tr}[\chi_i^{\Omega(m)}]$ has a deeper physical origin beyond local geometric quantities.

Analytical expression of $\text{Tr}[\chi_i]$.—Next, we provide a rigorous explanation for the novel and intriguing results obtained above. Due to the presence $\partial_{\varepsilon}f_k^0$, at zero temperature the integral in Eq. (3) actually is performed on the Fermi surface. Since $\text{Tr}[\chi_i^{(1)}] = -\chi_{i;jj}^{(3)} = -\text{Tr}[\chi_i^{(3)}]/3$, we start our analysis from $\text{Tr}[\chi_i^{(3)}]$, which can be rewritten as

$$\text{Tr}[\chi_i^{(3)}] = 3 \frac{e^3\tau}{(2\pi)^3\hbar^2} \oint_{\varepsilon=E_F} v_i \Omega_{\perp} dS, \quad (8)$$

where S denotes the Fermi surface, the subscript \perp represents the normal component of the corresponding quantities with respect to S , and the equations $\mathbf{v}_{\mathbf{k}} \cdot \boldsymbol{\Omega}_{\mathbf{k}} = v_{\perp} \Omega_{\perp}$ and $v_{\perp} = \partial_{k_{\perp}} \varepsilon / \hbar$ are used. For model (7), its dispersion is $\varepsilon = w_x k_x + \varepsilon_0$ with ε_0 denotes the dispersion without energy tilt. Then, one has $v_x = w_x / \hbar + v_{x,0}$ with $v_{x,0} = \partial_{k_x} \varepsilon_0 / \hbar$. Interestingly, the x -component of $\text{Tr}[\chi^{(3)}]$ becomes [see the Supplementary Material [85] for

details]

$$\begin{aligned} \text{Tr}[\chi_x^{(3)}] &= \frac{3e^3\tau}{(2\pi)^3\hbar^3} (w_x \oint \Omega_{\perp} dS + \oint \hbar v_{x,0} \Omega_{\perp} dS) \\ &= 9\eta w_x \mathcal{C}, \end{aligned} \quad (9)$$

with $\eta = \frac{e^3\tau}{12\pi^2\hbar^3}$ and \mathcal{C} the Chern number of the 2D Fermi surface, which is exactly the Chern number of the WP. Since the energy tilt along $k_{y(z)}$ is zero, one has $\text{Tr}[\chi_y^{(3)}] = \text{Tr}[\chi_z^{(3)}] = 0$ [85]. Besides, from Eq. 3, we have $\text{Tr}[\chi_i^{(2)}] = (\text{Tr}[\chi_x^{(3)}] + \text{Tr}[\chi_y^{(3)}] + \text{Tr}[\chi_z^{(3)}])/3$, indicating that $\text{Tr}[\chi_{x/y/z}^{(2)}] = 3\eta w_x \mathcal{C}$. Therefore, the PHE conductivity contributed by Berry curvature is

$$\text{Tr}[\chi_x^{\Omega}] = 9\eta w_x \mathcal{C}, \quad (10)$$

$$\text{Tr}[\chi_y^{\Omega}] = \text{Tr}[\chi_z^{\Omega}] = 3\eta w_x \mathcal{C}. \quad (11)$$

A more complicated calculation demonstrates that $\text{Tr}[\chi_i^{(4)}] = \text{Tr}[\chi_i^{(5)}]$, and the PHE conductivity contributed by orbital moment is [85]

$$\text{Tr}[\chi_x^m] = -(4 + 2\beta)\eta w_x \mathcal{C}, \quad (12)$$

$$\text{Tr}[\chi_y^m] = \text{Tr}[\chi_z^m] = 0, \quad (13)$$

with $\beta = [-2\alpha^3 + 3\alpha + 3(\alpha^2 - 1)\text{arctanh}\alpha]/\alpha^3$ and $\alpha = |w_x/v_1| < 1$ denoting the relative energy tilt. Obviously, β represents the deviation of $\text{Tr}[\chi_x^m]$ from a simple linear relationship with $w_x \mathcal{C}$. It rapidly approaches zero as w_x decreases, which can be inferred from the alternative expression of β : $\beta = \sum_{n=1}^{\infty} \frac{6\alpha^{2n}}{4n^2 + 8n + 3}$. The Eqs. (10-13) are the main results of this work, and is summarized in Table I. These results directly show that the PHE is highly nontrivial, and originates from the global topological quantities of the Fermi surface. Consequently, in contrast to various Hall effects, the PHE conductivity in magnetic Weyl semimetals are robust against many kinds of small perturbations, as shown in Fig. 3.

Lattice model.—Our results so far are obtained on the effective model around a WP. We point out that the PHE

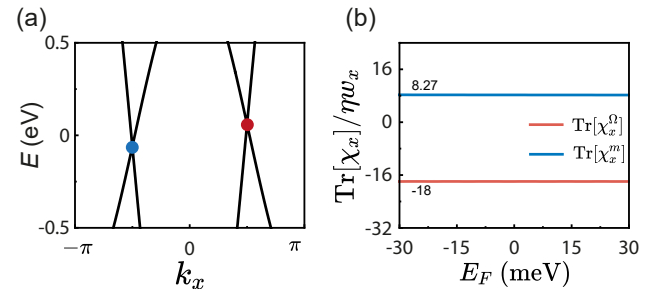


FIG. 4. (a) Band structure of the Weyl model (14). (b) Variation of the PHE conductivity with Fermi energy where the corresponding $\beta = 0.069$. We set $\tau = 0.1$ ps, $m = t = 1.5$ eV·Å, $w_x = 0.6$ eV·Å, $\Delta = 0.06$ eV·Å and $k_0 = \pi/2$ Å⁻¹.

plateau can persist in a realistic lattice model, and is almost precise when the Fermi energy is around WPs. Consider a minimal lattice models for topological magnetic Weyl semimetal, expressed as [86]

$$\begin{aligned} \mathcal{H}_3 = & [m(\cos k_y + \cos k_z - 2) - t(\cos k_x - \cos k_0)] \sigma_x \\ & - t \sin k_y \sigma_y - t \sin k_z \sigma_z + w_x (\cos k_0 - \cos k_x) \\ & + \Delta \sin k_x, \end{aligned} \quad (14)$$

where m , t and k_0 are model parameters, and w_x denotes the energy tilt. The band structure of the Weyl model (14) is plotted in Fig. 4(a), in which two tilted linear WPs with $|\mathcal{C}| = 1$ at $(\pm k_0, 0, 0)$ position can be observed when w_x is finite. Since the two WPs have both opposite energy tilt and Chern number, one can expect that the total PHE conductivity $\text{Tr}[\chi_i](\propto w_x \mathcal{C})$ from the two WPs would not be canceled but is added.

The numerically calculated PHE conductivities of model (14) as a function of E_F are plotted in Fig. 4(b). These conductivities continue to display a flat plateau and preserve their mutual proportional relationships, as revealed in Eqs. (10-13) and Table I. Moreover, the plateau values have now doubled due to the presence of two WPs.

Conclusions.— In conclusion, we demonstrate that the PHE conductivity can be directly related to the topological charge of WPs, and then features quantized plateau by varying many material parameters. Our work significantly advances the understanding of magnetotransport in magnetic Weyl semimetals, highlighting the crucial role of Chern number and energy tilt of the WPs, and providing an attractive prospect for future explorations on quantized Hall transport phenomena in topological materials.

This work was supported by the National Key R&D Program of China (Grant No. 2020YFA0308800), the NSF of China (Grants Nos. 12004035, 12234003 and 12321004) and the China Postdoctoral Science Foundation (Grants Nos. 2021TQ0043 and 2021M700437).

[1] D. Xiao, M.-C. Chang, and Q. Niu, Berry phase effects on electronic properties, *Rev. Mod. Phys.* **82**, 1959 (2010).
 [2] A. Bansil, H. Lin, and T. Das, Colloquium: Topological band theory, *Rev. Mod. Phys.* **88**, 021004 (2016).
 [3] Y. Yao, L. Kleinman, A. H. MacDonald, J. Sinova, T. Jungwirth, D.-s. Wang, E. Wang, and Q. Niu, First principles calculation of anomalous Hall conductivity in ferromagnetic bcc Fe, *Phys. Rev. Lett.* **92**, 037204 (2004).
 [4] I. Sodemann and L. Fu, Quantum nonlinear Hall effect induced by Berry curvature dipole in time-reversal invariant materials, *Phys. Rev. Lett.* **115**, 216806 (2015).
 [5] S.-Y. Xu, Q. Ma, H. Shen, V. Fatemi, S. Wu, T.-R. Chang, G. Chang, A. M. M. Valdivia, C.-K. Chan, Q. D. Gibson, *et al.*, Electrically switchable Berry curvature

dipole in the monolayer topological insulator WTe₂, *Nature Physics* **14**, 900 (2018).
 [6] Y. Zhang, Y. Sun, and B. Yan, Berry curvature dipole in Weyl semimetal materials: An ab initio study, *Phys. Rev. B* **97**, 041101 (2018).
 [7] X.-G. Ye, H. Liu, P.-F. Zhu, W.-Z. Xu, S. A. Yang, N. Shang, K. Liu, and Z.-M. Liao, Control over Berry curvature dipole with electric field in WTe₂, *Phys. Rev. Lett.* **130**, 016301 (2023).
 [8] H. Liu, J. Zhao, Y.-X. Huang, W. Wu, X.-L. Sheng, C. Xiao, and S. A. Yang, Intrinsic second-order anomalous Hall effect and its application in compensated antiferromagnets, *Phys. Rev. Lett.* **127**, 277202 (2021).
 [9] C. Wang, Y. Gao, and D. Xiao, Intrinsic nonlinear Hall effect in antiferromagnetic tetragonal CuMnAs, *Phys. Rev. Lett.* **127**, 277201 (2021).
 [10] H. Liu, J. Zhao, Y.-X. Huang, X. Feng, C. Xiao, W. Wu, S. Lai, W.-b. Gao, and S. A. Yang, Berry connection polarizability tensor and third-order hall effect, *Phys. Rev. B* **105**, 045118 (2022).
 [11] Z. Zhu, H. Liu, Y. Ge, Z. Zhang, W. Wu, C. Xiao, and S. A. Yang, Third-order charge transport in a magnetic topological semimetal, *Phys. Rev. B* **107**, 205120 (2023).
 [12] Y. Gao, S. A. Yang, and Q. Niu, Field induced positional shift of Bloch electrons and its dynamical implications, *Phys. Rev. Lett.* **112**, 166601 (2014).
 [13] C. Xiao, H. Liu, W. Wu, H. Wang, Q. Niu, and S. A. Yang, Intrinsic nonlinear electric spin generation in centrosymmetric magnets, *Phys. Rev. Lett.* **129**, 086602 (2022).
 [14] F. Piéchon, A. Raoux, J.-N. Fuchs, and G. Montambaux, Geometric orbital susceptibility: Quantum metric without Berry curvature, *Phys. Rev. B* **94**, 134423 (2016).
 [15] J.-W. Rhim, K. Kim, and B.-J. Yang, Quantum distance and anomalous Landau levels of flat bands, *Nature* **584**, 59 (2020).
 [16] J. Ahn, G.-Y. Guo, N. Nagaosa, and A. Vishwanath, Riemannian geometry of resonant optical responses, *Nature Physics* **18**, 290 (2022).
 [17] K. Das, S. Lahiri, R. B. Atencia, D. Culcer, and A. Agarwal, Intrinsic nonlinear conductivities induced by the quantum metric, *Phys. Rev. B* **108**, L201405 (2023).
 [18] L. Xiang, B. Wang, Y. Wei, Z. Qiao, and J. Wang, Linear displacement current solely driven by the quantum metric, *Phys. Rev. B* **109**, 115121 (2024).
 [19] C.-K. Chiu, J. C. Y. Teo, A. P. Schnyder, and S. Ryu, Classification of topological quantum matter with symmetries, *Rev. Mod. Phys.* **88**, 035005 (2016).
 [20] B. Xie, H.-X. Wang, X. Zhang, P. Zhan, J.-H. Jiang, M. Lu, and Y. Chen, Higher-order band topology, *Nature Reviews Physics* **3**, 520 (2021).
 [21] B. Bradlyn, L. Elcoro, J. Cano, M. G. Vergniory, Z. Wang, C. Felser, M. I. Aroyo, and B. A. Bernevig, Topological quantum chemistry, *Nature* **547**, 298 (2017).
 [22] H. C. Po, A. Vishwanath, and H. Watanabe, Symmetry-based indicators of band topology in the 230 space groups, *Nature communications* **8**, 50 (2017).
 [23] J. Kruthoff, J. de Boer, J. van Wezel, C. L. Kane, and R.-J. Slager, Topological classification of crystalline insulators through band structure combinatorics, *Phys. Rev. X* **7**, 041069 (2017).
 [24] D. Vanderbilt, *Berry phases in electronic structure theory: electric polarization, orbital magnetization and topological insulators* (Cambridge University Press, 2018).

- [25] B. A. Bernevig, *Topological insulators and topological superconductors* (Princeton university press, 2013).
- [26] S.-Q. SHEN, *Topological Insulators: Dirac Equation in Condensed Matter* (Springer, 2018).
- [27] Z. Du, H.-Z. Lu, and X. Xie, Nonlinear Hall effects, *Nature Reviews Physics* **3**, 744 (2021).
- [28] C. Xiao, Z. Z. Du, and Q. Niu, Theory of nonlinear hall effects: Modified semiclassics from quantum kinetics, *Phys. Rev. B* **100**, 165422 (2019).
- [29] S. Nandy and I. Sodemann, Symmetry and quantum kinetics of the nonlinear Hall effect, *Phys. Rev. B* **100**, 195117 (2019).
- [30] S. Lai, H. Liu, Z. Zhang, J. Zhao, X. Feng, N. Wang, C. Tang, Y. Liu, K. Novoselov, S. A. Yang, *et al.*, Third-order nonlinear Hall effect induced by the Berry-connection polarizability tensor, *Nature Nanotechnology* **16**, 869 (2021).
- [31] J. Wang, H. Zeng, W. Duan, and H. Huang, Intrinsic nonlinear Hall detection of the Néel vector for two-dimensional antiferromagnetic spintronics, *Phys. Rev. Lett.* **131**, 056401 (2023).
- [32] T. Nag, S. K. Das, C. Zeng, and S. Nandy, Third-order Hall effect in the surface states of a topological insulator, *Phys. Rev. B* **107**, 245141 (2023).
- [33] N. Wang, D. Kaplan, Z. Zhang, T. Holder, N. Cao, A. Wang, X. Zhou, F. Zhou, Z. Jiang, C. Zhang, *et al.*, Quantum-metric-induced nonlinear transport in a topological antiferromagnet, *Nature* **621**, 487 (2023).
- [34] A. Gao, Y.-F. Liu, J.-X. Qiu, B. Ghosh, T. V. Trevisan, Y. Onishi, C. Hu, T. Qian, H.-J. Tien, S.-W. Chen, *et al.*, Quantum metric nonlinear Hall effect in a topological antiferromagnetic heterostructure, *Science* **381**, 181 (2023).
- [35] D. Kaplan, T. Holder, and B. Yan, General nonlinear Hall current in magnetic insulators beyond the quantum anomalous Hall effect, *Nature communications* **14**, 3053 (2023).
- [36] L. Xiang, C. Zhang, L. Wang, and J. Wang, Third-order intrinsic anomalous Hall effect with generalized semiclassical theory, *Phys. Rev. B* **107**, 075411 (2023).
- [37] D. Ma, A. Arora, G. Vignale, and J. C. W. Song, Anomalous skew-scattering nonlinear hall effect and chiral photocurrents in \mathcal{PT} -symmetric antiferromagnets, *Phys. Rev. Lett.* **131**, 076601 (2023).
- [38] C. Xiao, W. Wu, H. Wang, Y.-X. Huang, X. Feng, H. Liu, G.-Y. Guo, Q. Niu, and S. A. Yang, Time-reversal-even nonlinear current induced spin polarization, *Phys. Rev. Lett.* **130**, 166302 (2023).
- [39] A. Kirikoshi and S. Hayami, Microscopic mechanism for intrinsic nonlinear anomalous Hall conductivity in non-collinear antiferromagnetic metals, *Phys. Rev. B* **107**, 155109 (2023).
- [40] L. Wang, J. Zhu, H. Chen, H. Wang, J. Liu, Y.-X. Huang, B. Jiang, J. Zhao, H. Shi, G. Tian, H. Wang, Y. Yao, D. Yu, Z. Wang, C. Xiao, S. A. Yang, and X. Wu, Orbital magneto-nonlinear anomalous Hall effect in Kagome magnet Fe_3Sn_2 , *Phys. Rev. Lett.* **132**, 106601 (2024).
- [41] K. Das, K. Ghorai, D. Culcer, and A. Agarwal, Nonlinear valley Hall effect, *Phys. Rev. Lett.* **132**, 096302 (2024).
- [42] Y. Fang, J. Cano, and S. A. A. Ghorashi, Quantum geometry induced nonlinear transport in altermagnets, *arXiv preprint arXiv:2310.11489* (2023).
- [43] Y.-X. Huang, C. Xiao, S. A. Yang, and X. Li, Scaling law for time-reversal-odd nonlinear transport, *arXiv preprint arXiv:2311.01219* (2023).
- [44] D. Kaplan, T. Holder, and B. Yan, Unification of nonlinear anomalous Hall effect and nonreciprocal magnetoresistance in metals by the quantum geometry, *Phys. Rev. Lett.* **132**, 026301 (2024).
- [45] B. Zhao, X. Yan, and A. B. Pakhomov, Anisotropic magnetoresistance and planar Hall effect in magnetic metal-insulator composite films, *Journal of Applied Physics* **81**, 5527 (1997).
- [46] P. He, S. S.-L. Zhang, D. Zhu, S. Shi, O. G. Heinonen, G. Vignale, and H. Yang, Nonlinear planar Hall effect, *Phys. Rev. Lett.* **123**, 016801 (2019).
- [47] V. A. Zyuzin, In-plane Hall effect in two-dimensional helical electron systems, *Phys. Rev. B* **102**, 241105 (2020).
- [48] R. Battilomo, N. Scopigno, and C. Ortix, Anomalous planar Hall effect in two-dimensional trigonal crystals, *Phys. Rev. Res.* **3**, L012006 (2021).
- [49] J. Cao, W. Jiang, X.-P. Li, D. Tu, J. Zhou, J. Zhou, and Y. Yao, In-plane anomalous Hall effect in \mathcal{PT} -symmetric antiferromagnetic materials, *Phys. Rev. Lett.* **130**, 166702 (2023).
- [50] Y.-X. Huang, X. Feng, H. Wang, C. Xiao, and S. A. Yang, Intrinsic nonlinear planar Hall effect, *Phys. Rev. Lett.* **130**, 126303 (2023).
- [51] Y. Wang, Z.-G. Zhu, and G. Su, Field-induced Berry connection and planar Hall effect in tilted Weyl semimetals (2023), [arXiv:2303.03579](https://arxiv.org/abs/2303.03579) [cond-mat.mes-hall].
- [52] J.-Y. Ba, Y.-M. Wang, H.-J. Duan, M.-X. Deng, and R.-Q. Wang, Nonlinear planar Hall effect induced by interband transitions: Application to surface states of topological insulators, *Phys. Rev. B* **108**, L241104 (2023).
- [53] Y.-X. Huang, Y. Wang, H. Wang, C. Xiao, X. Li, and S. A. Yang, Nonlinear current response of two-dimensional systems under in-plane magnetic field, *Phys. Rev. B* **108**, 075155 (2023).
- [54] H. Zheng, D. Zhai, C. Xiao, and W. Yao, Layer coherence origin of intrinsic Planar hall effect in 2D limit, *arXiv preprint arXiv:2402.17166* (2024).
- [55] L. Xiang and J. Wang, Intrinsic in-plane magnetononlinear hall effect in tilted weyl semimetals, *Phys. Rev. B* **109**, 075419 (2024).
- [56] H. Wang, Y.-X. Huang, H. Liu, X. Feng, J. Zhu, W. Wu, C. Xiao, and S. A. Yang, Orbital origin of the intrinsic planar hall effect, *Phys. Rev. Lett.* **132**, 056301 (2024).
- [57] J. Ge, D. Ma, Y. Liu, H. Wang, Y. Li, J. Luo, T. Luo, Y. Xing, J. Yan, D. Mandrus, H. Liu, X. C. Xie, and J. Wang, Unconventional Hall effect induced by Berry curvature, *National Science Review* **7**, 1879 (2020).
- [58] J. Zhong, J. Zhuang, and Y. Du, Recent progress on the planar hall effect in quantum materials, *Chinese Physics B* **32**, 047203 (2023).
- [59] S. Xu, H. Wang, X.-Y. Wang, Y. Su, P. Cheng, and T.-L. Xia, Planar Hall effect in the Dirac semimetal PdTe_2 , *arXiv e-prints*, [arXiv:1811.06767](https://arxiv.org/abs/1811.06767) (2018), [arXiv:1811.06767](https://arxiv.org/abs/1811.06767) [cond-mat.mtrl-sci].
- [60] M. Wu, G. Zheng, W. Chu, Y. Liu, W. Gao, H. Zhang, J. Lu, Y. Han, J. Zhou, W. Ning, and M. Tian, Probing the chiral anomaly by planar Hall effect in Dirac semimetal Cd_3As_2 nanoplates, *Phys. Rev. B* **98**, 161110 (2018).
- [61] Y. J. Wang, J. X. Gong, D. D. Liang, M. Ge, J. R. Wang, W. K. Zhu, and C. J. Zhang, Planar Hall effect in type-II Weyl semimetal WTe_2 , *arXiv e-prints*, [arXiv:1801.05929](https://arxiv.org/abs/1801.05929) (2018), [arXiv:1801.05929](https://arxiv.org/abs/1801.05929) [cond-mat.mtrl-sci].
- [62] R. Singha, S. Roy, A. Pariari, B. Satpati, and P. Mandal,

- Planar Hall effect in the type-II Dirac semimetal VAl_3 , *Phys. Rev. B* **98**, 081103 (2018).
- [63] N. Kumar, S. N. Guin, C. Felser, and C. Shekhar, Planar Hall effect in the Weyl semimetal GdPtBi , *Phys. Rev. B* **98**, 041103 (2018).
- [64] P. Li, C. Zhang, Y. Wen, L. Cheng, G. Nichols, D. G. Cory, G.-X. Miao, and X.-X. Zhang, Anisotropic planar Hall effect in the type-II topological Weyl semimetal WTe_2 , *Phys. Rev. B* **100**, 205128 (2019).
- [65] Sonika, S. Gangwar, N. S. Mehta, G. Sharma, and C. S. Yadav, Chiral anomaly and positive longitudinal magnetoresistance in the *type-ii* dirac semimetals $A_x\text{pdte}_2$ ($a = \text{Cu, Ag}$), *Phys. Rev. B* **108**, 245141 (2023).
- [66] L. Li, E. Yi, B. Wang, G. Yu, B. Shen, Z. Yan, and M. Wang, Higher-order oscillatory planar Hall effect in topological kagome metal, *npj Quantum Materials* **8**, 2 (2023).
- [67] L. Li, J. Cao, C. Cui, Z.-M. Yu, and Y. Yao, Planar Hall effect in topological Weyl and nodal-line semimetals, *Phys. Rev. B* **108**, 085120 (2023).
- [68] S. Nandy, G. Sharma, A. Taraphder, and S. Tewari, Chiral anomaly as the origin of the planar Hall effect in Weyl semimetals, *Phys. Rev. Lett.* **119**, 176804 (2017).
- [69] D. Ma, H. Jiang, H. Liu, and X. C. Xie, Planar Hall effect in tilted Weyl semimetals, *Phys. Rev. B* **99**, 115121 (2019).
- [70] A. Yamada and Y. Fuseya, Negative magnetoresistance and sign change of the planar Hall effect due to negative off-diagonal effective mass in Weyl semimetals, *Phys. Rev. B* **105**, 205207 (2022).
- [71] M.-X. Deng, H.-J. Duan, W. Luo, W. Y. Deng, R.-Q. Wang, and L. Sheng, Quantum oscillation modulated angular dependence of the positive longitudinal magnetoresistance and planar Hall effect in Weyl semimetals, *Phys. Rev. B* **99**, 165146 (2019).
- [72] M. Imran and S. Hershfield, Berry curvature force and Lorentz force comparison in the magnetotransport of Weyl semimetals, *Phys. Rev. B* **98**, 205139 (2018).
- [73] S. Woo, B. Min, and H. Min, Semiclassical magnetotransport including effects of Berry curvature and Lorentz force, *Phys. Rev. B* **105**, 205126 (2022).
- [74] G. Sharma, S. Nandy, and S. Tewari, Sign of longitudinal magnetoconductivity and the planar Hall effect in Weyl semimetals, *Phys. Rev. B* **102**, 205107 (2020).
- [75] B. Sadhukhan and T. Nag, Effect of chirality imbalance on Hall transport of PrRhC_2 , *Phys. Rev. B* **107**, L081110 (2023).
- [76] N. W. Ashcroft and N. D. Mermin, *Solid state physics* (Holt, Rinehart and Winston, 1976).
- [77] T. Liang, J. Lin, Q. Gibson, S. Kushwaha, M. Liu, W. Wang, H. Xiong, J. A. Sobota, M. Hashimoto, P. S. Kirchmann, Z.-X. Shen, R. J. Cava, and N. P. Ong, Anomalous Hall effect in ZrTe_5 , *Nature Physics* **14**, 451 (2018).
- [78] J. Zhou, W. Zhang, Y. C. Lin, J. Cao, Y. Zhou, W. Jiang, H. Du, B. Tang, J. Shi, B. Jiang, X. Cao, B. Lin, Q. Fu, C. Zhu, W. Guo, Y. Huang, Y. Yao, S. S. P. Parkin, J. Zhou, Y. Gao, Y. Wang, Y. Hou, Y. Yao, K. Suenaga, X. Wu, and Z. Liu, Heterodimensional superlattice with in-plane anomalous Hall effect, *Nature* **609**, 46 (2022).
- [79] Z.-M. Yu, Z. Zhang, G.-B. Liu, W. Wu, X.-P. Li, R.-W. Zhang, S. A. Yang, and Y. Yao, Encyclopedia of emergent particles in three-dimensional crystals, *Science Bulletin* **67**, 375 (2022).
- [80] A. A. Soluyanov, D. Gresch, Z. Wang, Q. Wu, M. Troyer, X. Dai, and B. A. Bernevig, Type-II Weyl semimetals, *Nature* **527**, 495 (2015).
- [81] Z.-M. Yu, Y. Yao, and S. A. Yang, Predicted unusual magnetoresponse in type-II Weyl semimetals, *Phys. Rev. Lett.* **117**, 077202 (2016).
- [82] J. Cao, C. Zeng, X.-P. Li, M. Wang, S. A. Yang, Z.-M. Yu, and Y. Yao, Low-Frequency Divergence of Circular Photomagnetic Effect in Topological Semimetals, *arXiv e-prints*, arXiv:2201.06243 (2022).
- [83] G.-B. Liu, Z. Zhang, Z.-M. Yu, S. A. Yang, and Y. Yao, Systematic investigation of emergent particles in type-III magnetic space groups, *Phys. Rev. B* **105**, 085117 (2022).
- [84] Z. Zhang, G.-B. Liu, Z.-M. Yu, S. A. Yang, and Y. Yao, Encyclopedia of emergent particles in type-IV magnetic space groups, *Phys. Rev. B* **105**, 104426 (2022).
- [85] See supplemental material for detailed derivations for the analytical expression of χ_i .
- [86] T. M. McCormick, I. Kimchi, and N. Trivedi, Minimal models for topological Weyl semimetals, *Phys. Rev. B* **95**, 075133 (2017).

Supplemental Material for “ Planar Hall Plateau in Magnetic Weyl Semimetals ”

Lei Li,^{1,2,*} Chaoxi Cui,^{1,2,*} Run-Wu Zhang,^{1,2} Zhi-Ming Yu,^{1,2,†} and Yugui Yao^{1,2,‡}

¹Centre for Quantum Physics, Key Laboratory of Advanced Optoelectronic Quantum Architecture and Measurement (MOE), School of Physics, Beijing Institute of Technology, Beijing, 100081, China

²Beijing Key Lab of Nanophotonics & Ultrafine Optoelectronic Systems, School of Physics, Beijing Institute of Technology, Beijing, 100081, China

I. DERIVATION OF THE PHE CONDUCTIVITY

A. Linear model

We begin with the linear WP model described by Eq. (5) in the main text, as it is simple and its PHE conductivity can be obtained directly. The energy dispersion of this linear WP is $\varepsilon_{\mathbf{k}} = w_x k_x \pm v_1 k$ with $k = \sqrt{k_x^2 + k_y^2 + k_z^2}$. For the conduction band, the Berry curvature and the orbital moment are $\mathbf{\Omega}_{\mathbf{k}} = -\text{Sign}(v_1)\mathbf{k}/(2k^3)$ and $\mathbf{m} = -\text{Sign}(v_1)ev_1\mathbf{k}/(2k^2\hbar)$, respectively. Specifically, we set $v_1 > 0$. Then we have $\mathbf{\Omega}_{\mathbf{k}} = -\mathbf{k}/(2k^3)$, $\mathbf{m} = -ev_1\mathbf{k}/(2k^2\hbar)$ and the Chern number $\mathcal{C} = -1$ for conduction band. Since the energy tilt of this WP is along the k_x direction, it is convenient to calculate the PHE conductivity in spherical coordinates, expressed as:

$$k_x = k \cos \theta, \quad k_y = k \sin \theta \cos \phi, \quad k_z = k \sin \theta \sin \phi. \quad (\text{S1})$$

In the zero-temperature limit, we have $\partial_\varepsilon f_k^0 = -\delta(\varepsilon - E_F)$, which implies that the integrals for all the PHE conductivities here are performed on the Fermi surface. Then, for $\chi_{x;jj}^{(3)}$, one has

$$\begin{aligned} \chi_{x;jj}^{(3)} &= -\frac{e^3\tau}{\hbar} \int \frac{d^3k}{(2\pi)^3} v_x (\mathbf{\Omega}_{\mathbf{k}} \cdot \mathbf{v}_{\mathbf{k}}) \frac{\partial f_0}{\partial \varepsilon} \\ &= \frac{e^3\tau}{\hbar^3} \int \frac{d^3k}{(2\pi)^3} \left(-\frac{k_x v_1^2}{2k^3} - \frac{v_1 w_x}{2k^2} - \frac{k_x^2 v_1 w_x}{2k^4} - \frac{k_x w_x^2}{2k^3} \right) \delta(v_1 k + k_x w_x - E_F) \\ &= \frac{e^3\tau}{\hbar^3} \frac{1}{(2\pi)^3} \int d\phi d\theta \sin \theta \frac{-\cos \theta v_1^2 - v_1 w_x - v_1 w_x \cos^2 \theta - w_x^2 \cos \theta}{2(v_1 + w_x \cos \theta)} \int dk (v_1 + w_x \cos \theta) \delta[k(v_1 + w_x \cos \theta) - E_F] \\ &= \frac{e^3\tau}{\hbar^3} \frac{1}{(2\pi)^3} \int_0^\pi d\theta [-\pi (w_x + v_1 \cos \theta) \sin \theta] \\ &= -\frac{e^3\tau w_x}{4\pi^2 \hbar^3} \\ &= 3\eta w_x \mathcal{C}, \end{aligned} \quad (\text{S2})$$

with $\eta = \frac{e^3\tau}{12\pi^2 \hbar^3}$. This naturally leads to the results in Table I in main text, namely,

$$\text{Tr}[\chi_x^{(3)}] = 9\eta w_x \mathcal{C}. \quad (\text{S3})$$

Similarly, for $\chi_{y;jj}^{(3)}$ and $\chi_{z;jj}^{(3)}$, one has

$$\begin{aligned} \chi_{y;jj}^{(3)} &= -\frac{e^3\tau}{\hbar} \int \frac{d^3k}{(2\pi)^3} v_y (\mathbf{\Omega}_{\mathbf{k}} \cdot \mathbf{v}_{\mathbf{k}}) \frac{\partial f_0}{\partial \varepsilon} \\ &= \frac{e^3\tau}{\hbar^3} \int \frac{d^3k}{(2\pi)^3} \left(-\frac{k_y v_1^2}{2k^3} - \frac{k_x k_y v_1 w_x}{2k^4} \right) \delta(v_1 k + k_x w_x - E_F) \\ &= \frac{e^3\tau}{\hbar^3} \frac{1}{(2\pi)^3} \int_0^\pi d\theta \int_0^{2\pi} d\phi \left(-\frac{1}{2} v_1 \sin^2 \theta \cos \phi \right) \\ &= 0, \end{aligned} \quad (\text{S4})$$

* These authors contributed equally to this work

† zhiming_yu@bit.edu.cn

‡ ygyao@bit.edu.cn

and

$$\begin{aligned}
\chi_{z;jj}^{(3)} &= -\frac{e^3\tau}{\hbar} \int \frac{d^3k}{(2\pi)^3} v_z (\boldsymbol{\Omega}_{\mathbf{k}} \cdot \mathbf{v}_{\mathbf{k}}) \frac{\partial f_0}{\partial \varepsilon} \\
&= \frac{e^3\tau}{\hbar^3} \int \frac{d^3k}{(2\pi)^3} \left(-\frac{k_z v_1^2}{2k^3} - \frac{k_x k_z v_1 w_x}{2k^4} \right) \delta(v_1 k + k_x w_x - E_F) \\
&= \frac{e^3\tau}{\hbar^3} \frac{1}{(2\pi)^3} \int_0^\pi d\theta \int_0^{2\pi} d\phi \left(-\frac{1}{2} v_1 \sin^2 \theta \sin \phi \right) \\
&= 0,
\end{aligned} \tag{S5}$$

indicating that

$$\text{Tr}[\chi_y^{(3)}] = \text{Tr}[\chi_z^{(3)}] = 0. \tag{S6}$$

According to the Eq. (3) in the main text, we also have

$$\text{Tr}[\chi_i^{(1)}] = -\chi_{i;jj}^{(3)}, \tag{S7}$$

$$\text{Tr}[\chi_i^{(2)}] = \chi_{x;jj}^{(3)} + \chi_{y;jj}^{(3)} + \chi_{z;jj}^{(3)} = 3\eta w_x \mathcal{C}. \tag{S8}$$

For the terms induced by the orbital moment, *i.e.*, $\text{Tr}[\chi_i^{(4)}]$ and $\text{Tr}[\chi_i^{(5)}]$, their expressions are more complex. Specifically, one has

$$\begin{aligned}
\text{Tr}[\chi_x^{(4)}] &= \sum_j \chi_{x;jj}^{(4)} \\
&= \sum_j \frac{e^2\tau}{\hbar} \int \frac{d^3k}{(2\pi)^3} v_x \partial_{k_j} m_j \frac{\partial f_0}{\partial \varepsilon} \\
&= -\frac{e^3\tau}{\hbar^3} \frac{1}{(2\pi)^3} \int_0^\pi d\theta \left[-\frac{\pi v_1 (w_x + v_1 \cos \theta) \sin \theta}{v_1 + w_x \cos \theta} \right] \\
&= \frac{e^3\tau}{\hbar^3} \frac{1}{(2\pi)^3} \int_0^\pi d\theta \left[\frac{\pi w_x (1 + \cos \theta / \alpha) \sin \theta}{1 + \alpha \cos \theta} \right] \\
&= \frac{e^3\tau}{\hbar^3} \frac{\pi w_x}{(2\pi)^3} \left[-\frac{\cos \theta}{\alpha^2} - \frac{(\alpha^2 - 1) \ln(1 + \alpha \cos \theta)}{\alpha^3} \right] \Big|_0^\pi \\
&= 2\eta w_x \frac{3\alpha + 3(\alpha^2 - 1) \text{arctanh } \alpha}{2\alpha^3} \\
&= 2\eta w_x + \frac{-2\alpha^3 + 3\alpha + 3(\alpha^2 - 1) \text{arctanh } \alpha}{\alpha^3} \eta w_x \\
&= (2 + \beta) \eta w_x \\
&= (-2 - \beta) \eta w_x \mathcal{C}
\end{aligned} \tag{S9}$$

where we have defined $\alpha = |w_x/v_1|$ and $\beta = \frac{-2\alpha^3 + 3\alpha + 3(\alpha^2 - 1) \text{arctanh } \alpha}{\alpha^3}$. For type-I WP, one has $\alpha < 1$. To further clarify the physical implications of the correction factor β , we rewrite it as $\beta = \sum_{n=1}^{\infty} \frac{6\alpha^{2n}}{4n^2 + 8n + 3}$, which shows the correction is induced by the relative energy tilt α , and rapidly approaches zero when α decreases.

We continue to calculate $\text{Tr}[\chi_y^{(4)}]$ and $\text{Tr}[\chi_z^{(4)}]$. One has

$$\begin{aligned}
\text{Tr}[\chi_y^{(4)}] &= \sum_j \chi_{y;jj}^{(4)} \\
&= \sum_j \frac{e^2\tau}{\hbar} \int \frac{d^3k}{(2\pi)^3} v_y \partial_{k_j} m_j \frac{\partial f_0}{\partial \varepsilon} \\
&= -\frac{e^3\tau}{\hbar^3} \frac{1}{(2\pi)^3} \int_0^\pi d\theta \int_0^{2\pi} d\phi \left[-\frac{v_1^2 \sin^2 \theta \cos \phi}{2(v_1 + w_x \cos \theta)} \right] \\
&= 0,
\end{aligned} \tag{S10}$$

and

$$\begin{aligned}
\text{Tr}[\chi_z^{(4)}] &= \sum_j \chi_{z;jj}^{(4)} \\
&= \sum_j \frac{e^2 \tau}{\hbar} \int \frac{d^3 k}{(2\pi)^3} v_z \partial_{k_j} m_j \frac{\partial f_0}{\partial \varepsilon} \\
&= -\frac{e^3 \tau}{\hbar^3} \frac{1}{(2\pi)^3} \int_0^\pi d\theta \int_0^{2\pi} d\phi \left[-\frac{v_1^2 \sin^2 \theta \sin \phi}{2(v_1 + w_x \cos \theta)} \right] \\
&= 0.
\end{aligned} \tag{S11}$$

Through similar derivation, we find that

$$\text{Tr}[\chi_i^{(5)}] = \text{Tr}[\chi_i^{(4)}]. \tag{S12}$$

B. Generic WP model

Then, we derive analytical expressions of the PHE conductivity $\text{Tr}[\chi_i^{(l)}]$ for a generic magnetic WP with arbitrary Chern number. The Hamiltonian of a generic magnetic WP with energy tilt can be described by the Eq. (7) in the main text, expressed as

$$\begin{aligned}
\mathcal{H} &= w_x k_x + \mathcal{H}_0(\mathbf{k}) \\
&= w_x k_x + \begin{bmatrix} v_1 k_x & c_+ k_+^n + c_- k_-^n \\ c_+ k_-^n + c_- k_+^n & -v_1 k_x \end{bmatrix}.
\end{aligned} \tag{S13}$$

Here, without loss of generality, we assume the energy tilt is along k_x direction, $\mathcal{H}_0(\mathbf{k})$ denotes a generic WP Hamiltonian without energy tilt. As shown below, the PHE conductivities discussed here is solely determined by the Chern number of the $\mathcal{H}_0(\mathbf{k})$, but is independent of the specific values of the parameters in $\mathcal{H}_0(\mathbf{k})$. The dispersion for \mathcal{H} is $\varepsilon_{\mathbf{k}} = w_x k_x + \varepsilon_0$ with ε_0 the dispersion of $\mathcal{H}_0(\mathbf{k})$.

Again, we firstly study the expression of $\text{Tr}[\chi_i^{(3)}]$, expressed as

$$\begin{aligned}
\text{Tr}[\chi_i^{(3)}] &= \sum_j \chi_{i;jj}^{(3)} = -\frac{3e^3 \tau}{\hbar} \int \frac{d^3 k}{(2\pi)^3} v_i (\boldsymbol{\Omega}_{\mathbf{k}} \cdot \mathbf{v}_{\mathbf{k}}) \frac{\partial f_0}{\partial \varepsilon} \\
&= \frac{3e^3 \tau}{(2\pi)^3 \hbar} \int v_i \Omega_{\perp} dS \int v_{\perp} \delta(\varepsilon - E_F) dk_{\perp} \\
&= \frac{3e^3 \tau}{(2\pi)^3 \hbar^2} \oint_{\varepsilon=E_F} v_i \Omega_{\perp} dS,
\end{aligned} \tag{S14}$$

where $\mathbf{v}_{\mathbf{k}} \cdot \boldsymbol{\Omega}_{\mathbf{k}} = v_{\perp} \Omega_{\perp}$ is adopted, k_{\perp} is the component of wave vector \mathbf{k} normal to the Fermi surface, and $v_{\perp} = \partial_{k_{\perp}} \varepsilon / \hbar$ is always positive for electron Fermi pocket. The x -component velocity can be divided into two parts: $v_x = w_x / \hbar + \partial_{k_x} \varepsilon_0 / \hbar = w_x / \hbar + v_{x,0}$, and the Eq. (S14) can be further transformed into

$$\begin{aligned}
\text{Tr}[\chi_x^{(3)}] &= \frac{3e^3 \tau}{(2\pi)^3 \hbar^3} \oint_{\varepsilon=E_F} (w_x + \hbar v_{x,0}) \Omega_{\perp} dS \\
&= 9\eta w_x \mathcal{C} + \frac{3e^3 \tau}{(2\pi)^3 \hbar^2} \oint_{\varepsilon=E_F} v_{x,0} \Omega_{\perp} dS,
\end{aligned} \tag{S15}$$

where the Chern number \mathcal{C} is given by the integral $\oint_{\varepsilon=E_F} \Omega_{\perp} dS = 2\pi \mathcal{C}$. Now, the task becomes to prove that the last term of Eq. (S15) equals zero.

For a two-level system, it is convenient to map the system from k -space into d -space, where $\mathcal{H}_0(\mathbf{k}) = \mathbf{d}(\mathbf{k}) \cdot \mathbf{s}$ with $\mathbf{s} = (\sigma_z, \sigma_x, \sigma_y)$, and d_1 , d_2 , and d_3 denoting the coefficients of \mathbf{s} ,

$$\begin{aligned}
d_1 &= v_1 k_x, \\
d_2 &= (k_y + k_z)^{n/2} \{c_+ \cos[n \arg(k_y + ik_z)] + c_- \cos[n \arg(k_y - ik_z)]\}, \\
d_3 &= -(k_y + k_z)^{n/2} \{c_+ \sin[n \arg(k_y + ik_z)] + c_- \sin[n \arg(k_y - ik_z)]\}
\end{aligned} \tag{S16}$$

In the d -space, the Berry curvature takes a simple form of $\boldsymbol{\Omega}^d = -\frac{1}{2} \frac{\mathbf{d}}{d^3}$. According to the expression of \mathcal{H} [Eq. (S13)], we also have $v_{x,0} = \partial_{k_x} \sqrt{d_1^2 + d_2^2 + d_3^2} / \hbar = \frac{\partial d_1}{\partial k_x} d_1 / (\hbar d) = v_1 d_1 / (\hbar d)$. The mapping from k -space to d -space satisfies a useful property: $\Omega_{\perp}^k dS^k = \boldsymbol{\Omega}^k \cdot d\mathbf{S}^k = \text{Sign}(\mathcal{C}) \boldsymbol{\Omega}^d \cdot d\mathbf{S}^d = \text{Sign}(\mathcal{C}) \Omega_{\perp}^d dS^d$, which is proofed in Sec. II. Then, the integral in the last term of Eq. (S15) becomes

$$\begin{aligned} \oint_{\varepsilon=E_F} v_{x,0} \Omega_{\perp} dS &= -\text{Sign}(\mathcal{C}) \times \frac{v_1}{\hbar} \oint_{d=d_F} \frac{d_1 \mathbf{d}}{2d^4} \cdot d\mathbf{S}^d \\ &= -\text{Sign}(\mathcal{C}) \times \frac{v_1}{\hbar} \int \nabla_{\mathbf{d}} \cdot \left(\frac{d_1 \mathbf{d}}{2d^4} \right) dV^d = 0, \end{aligned} \quad (\text{S17})$$

as the gradient $\nabla \cdot \left(\frac{d_i \mathbf{d}}{d^4} \right) = 0$ for $i = 1, 2$, and 3 . Thus, from Eq. (S15), it is easy to know that

$$\text{Tr}[\chi_x^{(3)}] = 9\eta w_x \mathcal{C}. \quad (\text{S18})$$

For $\text{Tr}[\chi_{y(z)}^{(3)}]$, we have

$$\text{Tr}[\chi_{y(z)}^{(3)}] = \frac{3e^3 \tau}{(2\pi)^3 \hbar^2} \oint_{\varepsilon=E_F} v_{y(z)}(k, \theta, \phi) \Omega_{\perp}(k, \theta, \phi) dS, \quad (\text{S19})$$

According to the WP Hamiltonian \mathcal{H} [Eq. (S13)], it is easy to find out that $v_{y(z)}(k, \theta, \phi) = -v_{y(z)}(k, \theta, \phi + \pi)$ and $\Omega_{\perp}(k, \theta, \phi) = \Omega_{\perp}(k, \theta, \phi + \pi)$. Thus, one has

$$\text{Tr}[\chi_y^{(3)}] = \text{Tr}[\chi_z^{(3)}] = 0. \quad (\text{S20})$$

Similarly, from Eq. (3) in the main text, one has

$$\text{Tr}[\chi_i^{(1)}] = -\frac{1}{3} \text{Tr}[\chi_i^{(3)}], \quad (\text{S21})$$

$$\text{Tr}[\chi_i^{(2)}] = 3\eta w_x \mathcal{C}. \quad (\text{S22})$$

Next, we study the expressions of $\text{Tr}[\chi_i^{(4)}]$ and $\text{Tr}[\chi_i^{(5)}]$, which are induced by the orbital moment \mathbf{m} . Considering the definitions of orbital moment and Berry curvature

$$\begin{aligned} m_{n,\gamma} &= -e\hbar \epsilon_{\alpha\beta\gamma} \text{Im} \sum_{m \neq n} \frac{v_{nm}^{\alpha} v_{mn}^{\beta}}{\varepsilon_n - \varepsilon_m}, \\ \Omega_{n,\gamma} &= -2\hbar^2 \epsilon_{\alpha\beta\gamma} \text{Im} \sum_{m \neq n} \frac{v_{nm}^{\alpha} v_{mn}^{\beta}}{(\varepsilon_n - \varepsilon_m)^2}. \end{aligned} \quad (\text{S23})$$

One finds that for the two-band WP model, these two quantities have a simple relation, i.e. $m_{n,\gamma} = \frac{e}{2\hbar} \Omega_{n,\gamma} (\varepsilon_n - \varepsilon_m)$. Therefore, we can rewrite the expression of $\chi_{i;jj}^{(4)}$ as

$$\chi_{i;jj}^{(4)} = -\frac{e^3 \tau}{2\hbar} \int [d\mathbf{k}] v_i (\varepsilon_c - \varepsilon_v) (\partial_{k_j} \Omega_{c,j}) \partial_{\varepsilon} f_k^0 - \frac{e^3 \tau}{2} \int [d\mathbf{k}] v_i \Omega_{c,j} (v_{c,j} - v_{v,j}) \partial_{\varepsilon} f_k^0, \quad (\text{S24})$$

where $\Omega_{c,j}$ is the Berry curvature of conduction band, $\varepsilon_{c/v}$ denote the dispersion of conduction (valence) band, and $v_{c(v),i} = \partial_{k_i} \varepsilon_{c(v)} / \hbar$. We also define $v_i \equiv v_{c,i}$ for simplification, as we focus on the system that is electron doped here. Notice that in the region that does not have singularity, the gradient of Berry curvature is zero, i.e., $\nabla \cdot \boldsymbol{\Omega}_n = \sum_j \partial_{k_j} \Omega_{n,j} = 0$. For WP model (S13), the velocity of conduction and valence band also has a simple relation $v_{c,j}(\mathbf{k}) = -v_{v,j}(\mathbf{k}) + 2\delta_{j,x} w_x / \hbar$. Then, we have

$$\begin{aligned} \text{Tr}[\chi_x^{(4)}] &= \sum_j \chi_{x;jj}^{(4)} \\ &= \frac{e^3 \tau}{2\hbar} \oint_{\varepsilon=E_F} v_x (\varepsilon_c - \varepsilon_v) (\nabla \cdot \boldsymbol{\Omega}_c) dS - e^3 \tau \int [d\mathbf{k}] v_x \sum_j \Omega_j (v_j - \delta_{j,x} w_x / \hbar) \partial_{\varepsilon} f_k^0 \\ &= -e^3 \tau \int [d\mathbf{k}] v_x (\mathbf{v}_k \cdot \boldsymbol{\Omega}_k) \partial_{\varepsilon} f_k^0 + \frac{e^3 \tau w_x}{\hbar} \int [d\mathbf{k}] v_x \Omega_x \partial_{\varepsilon} f_k^0 \\ &= -3\eta w_x \mathcal{C} + \frac{e^3 \tau w_x}{\hbar} \int [d\mathbf{k}] v_x \Omega_x \partial_{\varepsilon} f_k^0, \end{aligned} \quad (\text{S25})$$

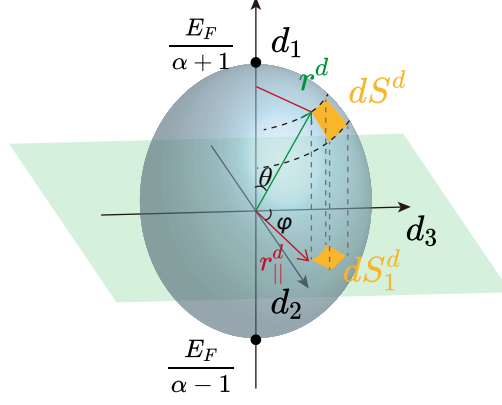


FIG. S1. The Fermi surface of the tilted WP in d -space.

where the result of $\text{Tr}[\chi_x^{(3)}]$ is used to obtain the last equation. For the second term in the last line of Eq. [S25], we have

$$\begin{aligned}
 \int [d\mathbf{k}] v_x \Omega_x \partial_\varepsilon f_k^0 &= -\frac{1}{(2\pi)^3 \hbar} \int dS dk_\perp v_x \Omega_x \partial_\varepsilon f_k^0 \\
 &= -\frac{1}{(2\pi)^3 \hbar} \int dS d\varepsilon \frac{1}{v_\perp} v_x \Omega_x \partial_\varepsilon f_k^0 \\
 &= \frac{1}{(2\pi)^3 \hbar^2} \oint_{\varepsilon=E_F} dS \frac{v_x \Omega_x}{v_\perp}. \tag{S26}
 \end{aligned}$$

Since the velocity \mathbf{v} at the Fermi surface is always perpendicular to the Fermi surface, one knows that $|\mathbf{v}| = v_\perp$, and the \mathbf{v} is parallel to the $d\mathbf{S}$. Thus, $\frac{v_x}{v_\perp} = \frac{dS^k}{dS^k}$, as $dS = |d\mathbf{S}|$, leading to $v_x \Omega_x / v_\perp dS = \Omega_x dS_x$.

It is also convenient to calculate Eq. (S26) in the d -space. As demonstrated in Sec. II, for the WP Hamiltonian \mathcal{H} [Eq. (S13)], we have $\Omega_x^k dS_x^k = \Omega_1^d dS_1^d$, and then

$$\int [d\mathbf{k}] v_x \Omega_x \partial_\varepsilon f_k^0 = \frac{1}{(2\pi)^3 \hbar^2} \oint_{\varepsilon=E_F} dS \frac{v_x \Omega_x}{v_\perp} = \frac{1}{(2\pi)^3 \hbar^2} \oint_{\varepsilon=E_F} \Omega_x dS_x = \frac{1}{(2\pi)^3 \hbar^2} \oint_{\varepsilon=E_F} \Omega_1^d dS_1^d. \tag{S27}$$

When $w_x \neq 0$, the WP Hamiltonian \mathcal{H} in d -space reads

$$\mathcal{H} = \alpha d_1 + \mathbf{d}(\mathbf{k}) \cdot \mathbf{s}, \tag{S28}$$

with $\alpha = w_x / v_1$. Then the Fermi surface of the WP in d -space is a ellipsoid (see Fig. S1), satisfying

$$\alpha d_1 + \sqrt{d_2^2 + (r_{\parallel}^d)^2} = E_F, \tag{S29}$$

with $r_{\parallel}^d = \sqrt{d_2^2 + d_3^2}$. From Fig. S1, one notices that

$$dS_1^d = r_{\parallel}^d d\phi^d dr^d = r_{\parallel}^d \frac{\partial r_{\parallel}^d}{\partial d_1} d\phi^d d(d_1), \tag{S30}$$

where r_{\parallel}^d can be easily obtained from Eq.(S29) *i.e.*, $r_{\parallel}^d = \sqrt{(E_F - \alpha d_1)^2 - d_2^2}$. The integration $\int \Omega_1^d dS_1^d$ then can be

transformed as

$$\begin{aligned}
\oint_{\varepsilon=E_F} \Omega_1^d dS_1^d &= \oint_{\varepsilon=E_F} \Omega_1^d r_{\parallel}^d \frac{\partial r_{\parallel}^d}{\partial d_1} d\phi^d d(d_1) \\
&= \text{Sign}(\mathcal{C}) \int_0^{2n\pi} d\phi^d \int_{\frac{E_F}{\alpha-1}}^{\frac{E_F}{\alpha+1}} d(d_1) \Omega_1^d r_{\parallel}^d \frac{\partial r_{\parallel}^d}{\partial d_1} \\
&= \pi \mathcal{C} \int_{\frac{E_F}{\alpha-1}}^{\frac{E_F}{\alpha+1}} d(d_1) \frac{d_1}{(E_F - \alpha d_1)^3} [(\alpha^2 - 1) d_1 - \alpha E_F] \\
&= 2\pi \mathcal{C} \frac{(\alpha^2 - 1) (\alpha - \text{arctanh } \alpha)}{\alpha^3}.
\end{aligned} \tag{S31}$$

Finally, we have

$$\begin{aligned}
\text{Tr}[\chi_x^{(4)}] &= -3\eta w_x \mathcal{C} + \frac{e^3 \tau w_x}{\hbar} \int [d\mathbf{k}] v_x \Omega_x \partial_{\varepsilon} f_k^0 \\
&= -3\eta w_x \mathcal{C} + \frac{e^3 \tau w_x}{\hbar} \times \frac{1}{(2\pi)^3 \hbar^2} \times 2\pi \mathcal{C} \frac{(\alpha^2 - 1) (\alpha - \text{arctanh } \alpha)}{\alpha^3} \\
&= (-2 - \beta) \eta w_x \mathcal{C}
\end{aligned} \tag{S32}$$

Besides, we have

$$\begin{aligned}
\text{Tr}[\chi_{y(z)}^{(4)}] &= \sum_j \chi_{y(z);jj}^{(4)} \\
&= -e^3 \tau \int [d\mathbf{k}] v_{y(z)} (\mathbf{v}_{\mathbf{k}} \cdot \mathbf{\Omega}_{\mathbf{k}}) \partial_{\varepsilon} f_k^0 + \frac{e^3 \tau w_x}{\hbar} \int [d\mathbf{k}] v_{y(z)} \Omega_x \partial_{\varepsilon} f_k^0 \\
&= \frac{e^3 \tau w_x}{\hbar} \int [d\mathbf{k}] v_{y(z)} \Omega_x \partial_{\varepsilon} f_k^0 \\
&= 0,
\end{aligned} \tag{S33}$$

as $v_{y(z)}(k, \theta, \phi) = -v_{y(z)}(k, \theta, \phi + \pi)$ and $\Omega_x(k, \theta, \phi) = \Omega_x(k, \theta, \phi + \pi)$.

For $\chi_{i;jj}^{(5)}$, we can see that it exactly equal to $\chi_{i;jj}^{(4)}$, due to the following equations

$$\begin{aligned}
\chi_{i;jj}^{(4)} &= -\frac{e^2 \tau}{(2\pi)^3 \hbar} \int d^3 k v_i (\partial_{k_j} m_j) (\partial_{\varepsilon} f_k^0) \\
&= -\frac{e^2 \tau}{(2\pi)^3 \hbar^2} \int dk_j dk_k \int dk_i \frac{\partial m_j}{\partial k_j} \frac{\partial f_k^0}{\partial k_i} \\
&= -\frac{e^2 \tau}{(2\pi)^3 \hbar^2} \int dk_j dk_k \int dk_i \left[\frac{\partial (f_k^0 \partial_{k_j} m_j)}{\partial k_i} - \frac{\partial^2 m_j}{\partial k_j \partial k_i} f_k^0 \right] \\
&= -\frac{e^2 \tau}{(2\pi)^3 \hbar^2} \int dk_j dk_k (f_k^0 \partial_{k_j} m_j) \Big|_{k_i=-\infty}^{k_i=\infty} + \frac{e^2 \tau}{(2\pi)^3 \hbar^2} \int dk_j dk_k \int dk_i \frac{\partial^2 m_j}{\partial k_j \partial k_i} f_k^0 \\
&= \frac{e^2 \tau}{(2\pi)^3 \hbar^2} \int dk_j dk_k \int dk_i \frac{\partial^2 m_j}{\partial k_j \partial k_i} f_k^0 \\
&= -\frac{e^2 \tau}{(2\pi)^3 \hbar^2} \int dk_j dk_k \int dk_i \frac{\partial m_j}{\partial k_i} \frac{\partial f_k^0}{\partial k_j} \\
&= -\frac{e^2 \tau}{(2\pi)^3 \hbar} \int d^3 k v_j (\partial_{k_i} m_j) (\partial_{\varepsilon} f_k^0) \\
&= \chi_{i;jj}^{(5)}.
\end{aligned} \tag{S34}$$

II. MAPPING FROM k -SPACE TO d -SPACE

In this section, we give the detail proof of the validity of the mapping from k -space to d -space in the integral. The WP Hamiltonian in k -space is

$$\mathcal{H} = w_x k_x + \begin{bmatrix} v_1 k_x & c_+ k_+^n + c_- k_-^n \\ c_+ k_-^n + c_- k_+^n & -v_1 k_x \end{bmatrix}, \quad (\text{S35})$$

and in d -space is

$$\mathcal{H} = \alpha d_1 + \mathbf{d}(\mathbf{k}) \cdot \mathbf{s}. \quad (\text{S36})$$

The Chern number of this WP is $\mathcal{C} = n \times \text{Sign}(v_1)$ for $|c_+| > |c_-|$ and is $\mathcal{C} = -n \times \text{Sign}(v_1)$ for $|c_+| < |c_-|$.

A. The first method

Technically, the mapping is exactly the integration by substitution, namely

$$\int_{\varphi(\mathbf{k})} f(\mathbf{d}) d\mathbf{d} = \int_{\mathbf{k}} f(\varphi(\mathbf{k})) \times |\det(J)| d\mathbf{k}, \quad (\text{S37})$$

where substitution function $(d_1, \dots, d_n) = \varphi(k_1, \dots, k_n)$, and $\det(J)$ denotes the determinant of the Jacobian matrix J of partial derivatives of φ at point \mathbf{k} . Consider a 2D surface defined in k -space S^k . The Berry curvature on S^k is

$$\Omega_{\perp}^k = \langle \partial_{k_1} u | \partial_{k_2} u \rangle - \langle \partial_{k_2} u | \partial_{k_1} u \rangle, \quad (\text{S38})$$

where k_1 and k_2 are two principal directions of surface S^k . Then we change it into d -space:

$$\begin{aligned} |\partial_{k_1} u\rangle &= \frac{\partial d_1}{\partial k_1} |\partial_{d_1} u\rangle + \frac{\partial d_2}{\partial k_1} |\partial_{d_2} u\rangle, \\ |\partial_{k_2} u\rangle &= \frac{\partial d_1}{\partial k_2} |\partial_{d_1} u\rangle + \frac{\partial d_2}{\partial k_2} |\partial_{d_2} u\rangle. \end{aligned} \quad (\text{S39})$$

After some simple algebra, we arrive at

$$\begin{aligned} \Omega_{\perp}^k &= \left(\frac{\partial d_1}{\partial k_1} \frac{\partial d_2}{\partial k_2} - \frac{\partial d_1}{\partial k_2} \frac{\partial d_2}{\partial k_1} \right) (\langle \partial_{d_1} u | \partial_{d_2} u \rangle - \langle \partial_{d_2} u | \partial_{d_1} u \rangle) \\ &= \begin{vmatrix} \frac{\partial d_1}{\partial k_1} & \frac{\partial d_1}{\partial k_2} \\ \frac{\partial d_2}{\partial k_1} & \frac{\partial d_2}{\partial k_2} \end{vmatrix} \Omega_{\perp}^d \\ &= \det(J) \Omega_{\perp}^d, \end{aligned} \quad (\text{S40})$$

with J the Jacobian matrix. Thus, one has

$$\mathbf{\Omega}^d \cdot d\mathbf{S}^d = \Omega_{\perp}^d dS^d = \Omega_{\perp}^d \times |\det(J)| dS^k = \text{Sign}[\det(J)] \Omega_{\perp}^k dS^k = \text{Sign}[\det(J)] \mathbf{\Omega}^k \cdot d\mathbf{S}^k, \quad (\text{S41})$$

and

$$\int_{\varphi(\mathbf{k})} \mathbf{\Omega}^d \cdot d\mathbf{S}^d = \int_{\mathbf{k}} \text{Sign}[\det(J)] \mathbf{\Omega}^k \cdot d\mathbf{S}^k. \quad (\text{S42})$$

For the WP Hamiltonian in Eqs. (S35) and (S36), we have

$$\int_{\varphi(\mathbf{k})} \mathbf{\Omega}^d \cdot d\mathbf{S}^d = \int_{\varphi(\mathbf{k})} \Omega_{\perp}^d dS^d = \int_0^{\pi} d\theta \int_0^{2n\pi} d\phi^d (r^d)^2 \Omega_{\perp}^d = \text{Sign}(\mathcal{C}) \int_{\mathbf{k}} \mathbf{\Omega}^k \cdot d\mathbf{S}^k. \quad (\text{S43})$$

Besides, for the WP Hamiltonian in Eqs. (S35) and (S36), one notice that d_1 is only a function of k_x , while d_2 and d_3 are only functions of k_y and k_z . This means that $dS_x^k = dk_y dk_z$ and $dS_1^d = dd_2 dd_3$. Thus, similar to the above derivation, we have

$$\begin{aligned} \Omega_x^k &= \langle \partial_{k_y} u | \partial_{k_z} u \rangle - \langle \partial_{k_z} u | \partial_{k_y} u \rangle, \\ |\partial_{k_y} u\rangle &= \frac{\partial d_2}{\partial k_y} |\partial_{d_2} u\rangle + \frac{\partial d_3}{\partial k_y} |\partial_{d_3} u\rangle, & |\partial_{k_z} u\rangle &= \frac{\partial d_2}{\partial k_z} |\partial_{d_2} u\rangle + \frac{\partial d_3}{\partial k_z} |\partial_{d_3} u\rangle. \end{aligned} \quad (\text{S44})$$

and

$$\Omega_x^k = \begin{vmatrix} \frac{\partial d_2}{\partial k_y} & \frac{\partial d_2}{\partial k_z} \\ \frac{\partial d_3}{\partial k_y} & \frac{\partial d_3}{\partial k_z} \end{vmatrix} \Omega_1^d = \det(J') \Omega_\perp^d, \quad (\text{S45})$$

with J' the Jacobian matrix. Thus, one has

$$\Omega_1^d dS_1^d = \Omega_1^d \times |\det(J')| dS_x^k = \text{Sign}[\det(J')] \Omega_x^k dS_x^k. \quad (\text{S46})$$

According to \mathcal{H} [Eq. (S13)] and Eq. (S16), $\det(J') = n^2(c_-^2 - c_+^2)(k_y^2 + k_z^2)^{n-1}$. Then, $\text{Sign}[\det(J')]$ is +1 when $|c_+| < |c_-|$, and is -1, when $|c_+| > |c_-|$.

B. The second method

In two-band systems, we defined d -space by $\mathcal{H}_0(\mathbf{k}) = \mathbf{d}(\mathbf{k}) \cdot \boldsymbol{\sigma}$ and $\mathbf{d}(\mathbf{k})$ is a vector in d -space. Consider a surface in k -space, denoted as S^k and its mapping in d -space is S^d . Then, consider four states on surface S^k : $|A\rangle, |B\rangle, |C\rangle$ and $|D\rangle$ which is very close to a point \mathbf{k}_0 . The Berry phase γ for the loop $ABCD$ is

$$\gamma = -\text{Arg} \langle A|\bar{B}\rangle \langle B|\bar{C}\rangle \langle C|\bar{D}\rangle \langle D|\bar{A}\rangle. \quad (\text{S47})$$

Supporting the area surrounded by loop $ABCD$ is ΔS^k and the Berry curvature at k_0 in S^k is Ω_\perp^k , we can also express Berry phase as the integral of Berry curvature and in a enough small area, it reduces to

$$\gamma \approx \Omega_\perp^k \cdot \Delta S^k. \quad (\text{S48})$$

Then we consider $|A\rangle, |B\rangle, |C\rangle$ and $|D\rangle$ in d -space. As the absolute value of Berry phase doesn't depend on parameter space, it is also $|\gamma|$. However, Berry curvature and surrounding area depend on parameter space, and respectively becomes Ω_\perp^d and ΔS^d . Then, we have

$$|\gamma| \approx \Omega_\perp^d \cdot \Delta S^d, \quad (\text{S49})$$

When the area is small enough, $\Delta S \rightarrow dS$ and we get

$$|\Omega_\perp^d \cdot dS^d| = |\Omega_\perp^k \cdot dS^k|. \quad (\text{S50})$$

This also means that when we proceed a mapping from one space to another, the flux of Berry curvature for a certain surface is unchanged.